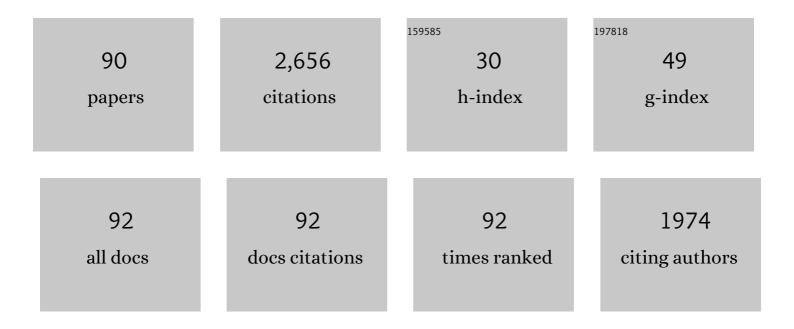
Siobhan A Wilson

List of Publications by Year in descending order

Source: https://exaly.com/author-pdf/2805995/publications.pdf Version: 2024-02-01



#	Article	IF	CITATIONS
1	Carbon Dioxide Fixation within Mine Wastes of Ultramafic-Hosted Ore Deposits: Examples from the Clinton Creek and Cassiar Chrysotile Deposits, Canada. Economic Geology, 2009, 104, 95-112.	3.8	201
2	Carbon Mineralization: From Natural Analogues to Engineered Systems. Reviews in Mineralogy and Geochemistry, 2013, 77, 305-360.	4.8	174
3	Verifying and quantifying carbon fixation in minerals from serpentine-rich mine tailings using the Rietveld method with X-ray powder diffraction data. American Mineralogist, 2006, 91, 1331-1341.	1.9	140
4	Serpentinite Carbonation for CO2 Sequestration. Elements, 2013, 9, 115-121.	0.5	123
5	Biologically induced mineralization of dypingite by cyanobacteria from an alkaline wetland near Atlin, British Columbia, Canada. Geochemical Transactions, 2007, 8, 13.	0.7	119
6	The hydromagnesite playas of Atlin, British Columbia, Canada: A biogeochemical model for CO2 sequestration. Chemical Geology, 2009, 260, 286-300.	3.3	114
7	Offsetting of CO2 emissions by air capture in mine tailings at the Mount Keith Nickel Mine, Western Australia: Rates, controls and prospects for carbon neutral mining. International Journal of Greenhouse Gas Control, 2014, 25, 121-140.	4.6	113
8	lsotopic Disequilibrium during Uptake of Atmospheric CO ₂ into Mine Process Waters: Implications for CO ₂ Sequestration. Environmental Science & Technology, 2010, 44, 9522-9529.	10.0	90
9	Microbially Mediated Mineral Carbonation: Roles of Phototrophy and Heterotrophy. Environmental Science & Technology, 2011, 45, 9061-9068.	10.0	84
10	Subarctic Weathering of Mineral Wastes Provides a Sink for Atmospheric CO ₂ . Environmental Science & Technology, 2011, 45, 7727-7736.	10.0	69
11	Reconstructing <i>Rangea</i> : new discoveries from the Ediacaran of southern Namibia. Journal of Paleontology, 2013, 87, 1-15.	0.8	66
12	Reactive Transport Modeling of Natural Carbon Sequestration in Ultramafic Mine Tailings. Vadose Zone Journal, 2012, 11, vzj2011.0053.	2.2	63
13	Quantifying carbon fixation in trace minerals from processed kimberlite: A comparative study of quantitative methods using X-ray powder diffraction data with applications to the Diavik Diamond Mine, Northwest Territories, Canada. Applied Geochemistry, 2009, 24, 2312-2331.	3.0	62
14	Strategizing Carbon-Neutral Mines: A Case for Pilot Projects. Minerals (Basel, Switzerland), 2014, 4, 399-436.	2.0	58
15	Increased thermal stability of nesquehonite (MgCO3·3H2O) in the presence of humidity and CO2: Implications for low-temperature CO2 storage. International Journal of Greenhouse Gas Control, 2015, 39, 366-376.	4.6	53
16	A depositional model for hydromagnesite–magnesite playas near Atlin, British Columbia, Canada. Sedimentology, 2014, 61, 1701-1733.	3.1	50
17	Microbially Accelerated Carbonate Mineral Precipitation as a Strategy for in Situ Carbon Sequestration and Rehabilitation of Asbestos Mine Sites. Environmental Science & Technology, 2016, 50, 1419-1427.	10.0	50
18	Mineral phosphorus drives glacier algal blooms on the Greenland Ice Sheet. Nature Communications, 2021, 12, 570.	12.8	50

#	Article	IF	CITATIONS
19	Potential for offsetting diamond mine carbon emissions through mineral carbonation of processed kimberlite: an assessment of De Beers mine sites in South Africa and Canada. Mineralogy and Petrology, 2018, 112, 755-765.	1.1	47
20	Stratigraphy, palaeontology and geochemistry of the late Neoproterozoic Aar Member, southwest Namibia: Reflecting environmental controls on Ediacara fossil preservation during the terminal Proterozoic in African Gondwana. Precambrian Research, 2013, 238, 214-232.	2.7	45
21	Ancient micrometeorites suggestive of an oxygen-rich Archaean upper atmosphere. Nature, 2016, 533, 235-238.	27.8	45
22	Accelerating Mineral Carbonation in Ultramafic Mine Tailings via Direct CO2 Reaction and Heap Leaching with Potential for Base Metal Enrichment and Recovery. Economic Geology, 2020, 115, 303-323.	3.8	45
23	Hydrotalcites and hydrated Mg-carbonates as carbon sinks in serpentinite mineral wastes from the Woodsreef chrysotile mine, New South Wales, Australia: Controls on carbonate mineralogy and efficiency of CO2 air capture in mine tailings. International Journal of Greenhouse Gas Control, 2018, 79. 38-60.	4.6	42
24	Modern carbonate microbialites from an asbestos open pit pond, Yukon, Canada. Geobiology, 2011, 9, 180-195.	2.4	40
25	Gas–Solid Reactions: Theory, Experiments and Case Studies Relevant to Earth and Planetary Processes. Reviews in Mineralogy and Geochemistry, 2018, 84, 1-56.	4.8	39
26	Fate of transition metals during passive carbonation of ultramafic mine tailings via air capture with potential for metal resource recovery. International Journal of Greenhouse Gas Control, 2018, 71, 155-167.	4.6	37
27	Investigation of the H7 ordinary chondrite, Watson 012: Implications for recognition and classification of Type 7 meteorites. Geochimica Et Cosmochimica Acta, 2014, 134, 175-196.	3.9	34
28	Production of magnesium-rich solutions by acid leaching of chrysotile: A precursor to field-scale deployment of microbially enabled carbonate mineral precipitation. Chemical Geology, 2015, 413, 119-131.	3.3	33
29	Magnesite formation in playa environments near Atlin, British Columbia, Canada. Geochimica Et Cosmochimica Acta, 2019, 255, 1-24.	3.9	33
30	Experimental Deployment of Microbial Mineral Carbonation at an Asbestos Mine: Potential Applications to Carbon Storage and Tailings Stabilization. Minerals (Basel, Switzerland), 2017, 7, 191.	2.0	31
31	The crystal structure of stichtite, re-examination of barbertonite, and the nature of polytypism in MgCr hydrotalcites. American Mineralogist, 2011, 96, 179-187.	1.9	30
32	Changes in Crystallinity and Tracer-Isotope Distribution of Goethite during Fe(II)-Accelerated Recrystallization. ACS Earth and Space Chemistry, 2018, 2, 1271-1282.	2.7	28
33	Nesquehonite sequesters transition metals and CO2 during accelerated carbon mineralisation. International Journal of Greenhouse Gas Control, 2016, 55, 73-81.	4.6	24
34	Microbial Populations of Stony Meteorites: Substrate Controls on First Colonizers. Frontiers in Microbiology, 2017, 8, 1227.	3.5	22
35	Evaluating feedstocks for carbon dioxide removal by enhanced rock weathering and CO2 mineralization. Applied Geochemistry, 2021, 129, 104955.	3.0	21
36	Effects of Curing Environment on the Strength and Mineralogy of Lime-GCBS–Treated Acid Sulphate Soils. Journal of Materials in Civil Engineering, 2014, 26, 1003-1008.	2.9	20

#	Article	IF	CITATIONS
37	Formation of gypsum and bassanite by cation exchange reactions in the absence of freeâ€liquid H ₂ O: Implications for Mars. Journal of Geophysical Research, 2011, 116, .	3.3	19
38	Stability of Mg-sulfate minerals in the presence of smectites: Possible mineralogical controls on H2O cycling and biomarker preservation on Mars. Geochimica Et Cosmochimica Acta, 2012, 96, 120-133.	3.9	19
39	Field-based accounting of CO ₂ sequestration in ultramafic mine wastes using portable X-ray diffraction. American Mineralogist, 2017, 102, 1302-1310.	1.9	19
40	Critical metals in the critical zone: controls, resources and future prospectivity of regolith-hosted rare earth elements. Australian Journal of Earth Sciences, 2017, 64, 1045-1054.	1.0	19
41	Comparison of Rietveld-compatible structureless fitting analysis methods for accurate quantification of carbon dioxide fixation in ultramafic mine tailings. American Mineralogist, 2018, 103, 1649-1662.	1.9	19
42	The decomposition of konyaite: importance in CO2 fixation in mine tailings. Mineralogical Magazine, 2010, 74, 903-917.	1.4	17
43	Enhanced silicate weathering is not limited by silicic acid saturation. Proceedings of the National Academy of Sciences of the United States of America, 2011, 108, E41; author reply E42.	7.1	17
44	Direct measurement of CO2 drawdown in mine wastes and rock powders: Implications for enhanced rock weathering. International Journal of Greenhouse Gas Control, 2022, 113, 103554.	4.6	15
45	Rapid immobilisation of U(VI) by Eucalyptus bark: Adsorption without reduction. Applied Geochemistry, 2018, 96, 1-10.	3.0	13
46	Tiny particles building huge ore deposits – Particle-based crystallisation in banded iron formation-hosted iron ore deposits (Hamersley Province, Australia). Ore Geology Reviews, 2019, 104, 160-174.	2.7	13
47	Quantitative Mineral Mapping of Drill Core Surfaces I: A Method for <i>µ</i> XRF Mineral Calculation and Mapping of Hydrothermally Altered, Fine-Grained Sedimentary Rocks from a Carlin-Type Gold Deposit. Economic Geology, 2021, 116, 803-819.	3.8	12
48	Chromium Reaction Mechanisms for Speciation using Synchrotron in-Situ High-Temperature X-ray Diffraction. Environmental Science & Technology, 2015, 49, 8246-8253.	10.0	11
49	Contribution to the crystallography of hydrotalcites: the crystal structures of woodallite and takovite. Journal of Geosciences (Czech Republic), 2013, , 273-279.	0.6	10
50	First non-destructive internal imaging of Rangea, an icon of complex Ediacaran life. Precambrian Research, 2017, 299, 303-308.	2.7	10
51	Evaluation of meteorites as habitats for terrestrial microorganisms: Results from the Nullarbor Plain, Australia, a Mars analogue site. Geochimica Et Cosmochimica Acta, 2017, 215, 1-16.	3.9	10
52	High Survivability of Micrometeorites on Mars: Sites With Enhanced Availability of Limiting Nutrients. Journal of Geophysical Research E: Planets, 2019, 124, 1802-1818.	3.6	10
53	Mineralisation of atmospheric CO2 in hydromagnesite in ultramafic mine tailings – Insights from Mg isotopes. Geochimica Et Cosmochimica Acta, 2021, 309, 191-208.	3.9	10
54	Problem Solving with the TOPAS Macro Language: Corrections and Constraints in Simulated Annealing and Rietveld Refinement. Materials Science Forum, 2010, 651, 11-25.	0.3	9

#	Article	IF	CITATIONS
55	Improvement of acid sulfate soils using lime-activated slag. Proceedings of the Institution of Civil Engineers: Ground Improvement, 2014, 167, 235-248.	1.0	9
56	Time-Dependent Strength and Mineralogy of Lime-GGBS Treated Naturally Occurring Acid Sulfate Soils. Journal of Materials in Civil Engineering, 2016, 28, .	2.9	9
57	Iron isotope geochemistry and mineralogy of jarosite in sulfur-rich sediments. Geochimica Et Cosmochimica Acta, 2020, 270, 282-295.	3.9	9
58	Non classical crystallization of very high magnesium calcite and magnesite in the Coorong Lakes, Australia. Sedimentology, 2022, 69, 2246-2266.	3.1	9
59	Cation Exchange in Smectites as a New Approach to Mineral Carbonation. Frontiers in Climate, 0, 4, .	2.8	9
60	9. Carbon Mineralization: From Natural Analogues to Engineered Systems. , 2013, , 305-360.		8
61	Colloidal origin of microbands in banded iron formations. Geochemical Perspectives Letters, 0, , 43-49.	5.0	7
62	Angastonite, CaMgAl2(PO4)2(OH)4·7H2O: a new phosphate mineral from Angaston, South Australia. Mineralogical Magazine, 2008, 72, 1011-1020.	1.4	6
63	Tellurium biogeochemical transformation and cycling in a metalliferous semi-arid environment. Geochimica Et Cosmochimica Acta, 2022, 321, 265-292.	3.9	6
64	Carbon accounting of mined landscapes, and deployment of a geochemical treatment system for enhanced weathering at Woodsreef Chrysotile Mine, NSW, Australia. Journal of Geochemical Exploration, 2021, 220, 106655.	3.2	5
65	A preliminary report on new Ediacaran fossils from Iran. Alcheringa, 2018, 42, 230-243.	1.2	5
66	Regrowth of arsenate–sulfate efflorescences on processing plant walls at the Ottery arsenic–tin mine, New South Wales, Australia: Implications for arsenic mobility and remediation of mineral processing sites. Applied Geochemistry, 2017, 79, 91-106.	3.0	4
67	Analysis of the Potential for Negative CO2 Emission Mine Sites through Bacteria-mediated Carbon Mineralisation: Evidence from Australia. Energy Procedia, 2017, 114, 6124-6132.	1.8	4
68	Unlocking the potential of hydraulic fracturing flowback and produced water for CO2 removal via mineral carbonation. Applied Geochemistry, 2022, 142, 105345.	3.0	4
69	Trace Elemental Partitioning on Clays Derived From Hydrothermal Muds of the El Tatio Geyser Field, Chile. Journal of Geophysical Research: Solid Earth, 2021, 126, e2020JB021422.	3.4	3
70	Effects of salinity on the leaching of ionic species from hydrocarbon target formations during hydraulic fracturing. Chemical Geology, 2022, 591, 120718.	3.3	3
71	Mineral Diversity on Europa: Exploration of Phases Formed in the MgSO ₄ –H ₂ SO ₄ –H ₂ O Ternary. ACS Earth and Space Chemistry, 2021, 5, 1716-1725.	2.7	2
72	Preservation of Terrestrial Microorganisms and Organics Within Alteration Products of Chondritic Meteorites from the Nullarbor Plain, Australia. Astrobiology, 2022, 22, 399-415.	3.0	2

#	Article	IF	CITATIONS
73	Accelerating mineral carbonation in hydraulic fracturing flowback and produced water using CO2-rich gas. Applied Geochemistry, 2022, 143, 105380.	3.0	2
74	Eukaryotic Colonization of Micrometer-Scale Cracks in Rocks: A "Microfluidics―Experiment Using Naturally Weathered Meteorites from the Nullarbor Plain, Australia. Astrobiology, 2020, 20, 364-374.	3.0	1
75	Mineral carbonation at Venetia and Gahcho Ku \tilde{A}^{0} diamond mines: Characterization of the highly reactive clay fraction. , 2021, , .		1
76	1. Gas–Solid Reactions: Theory, Experiments and Case Studies Relevant to Earth and Planetary Processes. , 2018, , 1-56.		0
77	The influence of invertebrate faecal material on compositional heterogeneity, diagenesis and trace metal distribution in the Ogeechee River estuary, Georgia, USA. Sedimentology, 2021, 68, 788-804.	3.1	0
78	New Perspectives on Carbonate Mineral Behaviour for Carbon Accounting and Carbon Utilization. , 2020, , .		0
79	Transition Metal Mobility and Partitioning in Weathered Tailings, Serpentinite and Skarn from the Lord Brassey Mine, Tasmania, Australia. , 2020, , .		О
80	Predicting CO ₂ Mineralization in Mine Residues: Insights from Leaching and Geochemical Modeling. , 2020, , .		0
81	Non-Classical Crystallization of Anhydrous Ca and Mg Carbonates from the Coorong Lakes, Australia. , 2020, , .		Ο
82	Direct measurement of CO ₂ fluxes into kimberlite residues and powdered rocks: Implications for enhanced weathering. , 2021, , .		0
83	Partitioning of Fe during carbonation of Fe-rich brucite. , 2021, , .		Ο
84	Quantifying the potential for mineral carbonation of processed kimberlite with the Rietveld-PONKCS method. , 2021, , .		0
85	Cation Exchange: A New Strategy for Mineral Carbonation of Smectite-Rich Kimberlites. , 2020, , .		Ο
86	Enhanced Weathering and Carbonation of Kimberlite Residues from South African Mines. , 2020, , .		0
87	Magnesium Isotope Signatures of Hydrotalcite Supergroup Minerals during Weathering and Carbonation of Ultramafic Mineral Wastes. , 2020, , .		0
88	Carbonation of Hydraulic Fracturing Flowback and Produced Water for Carbon Capture, Utilization and Storage. , 2020, , .		0
89	Migration of Transition Metals and Potential for Mineral Carbonation during Acid Leaching of Kimberlite Mine Tailings. , 2020, , .		0
90	Transition Metal Mobility and Recovery from Weathered Serpentinite and Serpentinite Skarn Tailings from Lord Brassey Mine, Australia and Record Ridge, British Columbia, Canada. , 2021, , .		0